



National Library
of Canada

Bibliothèque nationale
du Canada

Canadian Theses Service

Service des thèses canadiennes

Ottawa, Canada
K1A 0N4

NOTICE

The quality of this microform is heavily dependent upon the quality of the original thesis submitted for microfilming. Every effort has been made to ensure the highest quality of reproduction possible.

If pages are missing, contact the university which granted the degree.

Some pages may have indistinct print especially if the original pages were typed with a poor typewriter ribbon or if the university sent us an inferior photocopy.

Reproduction in full or in part of this microform is governed by the Canadian Copyright Act, R.S.C. 1970, c. C-30, and subsequent amendments.

AVIS

La qualité de cette microforme dépend grandement de la qualité de la thèse soumise au microfilmage. Nous avons tout fait pour assurer une qualité supérieure de reproduction.

S'il manque des pages, veuillez communiquer avec l'université qui a conféré le grade.

La qualité d'impression de certaines pages peut laisser à désirer, surtout si les pages originales ont été dactylographiées à l'aide d'un ruban usé ou si l'université nous a fait parvenir une photocopie de qualité inférieure.

La reproduction, même partielle, de cette microforme est soumise à la Loi canadienne sur le droit d'auteur, SRC 1970, c. C-30, et ses amendements subséquents.

Permission has been granted to the National Library of Canada to microfilm this thesis and to lend or sell copies of the film.

The author (copyright owner) has reserved other publication rights, and neither the thesis nor extensive extracts from it may be printed or otherwise reproduced without his/her written permission.

L'autorisation a été accordée à la Bibliothèque nationale du Canada de microfilmer cette thèse et de prêter ou de vendre des exemplaires du film.

L'auteur (titulaire du droit d'auteur) se réserve les autres droits de publication; ni la thèse ni de longs extraits de celle-ci ne doivent être imprimés ou autrement reproduits sans son autorisation écrite.

ISBN 0-315-53248-3

THE BOUNDARY ELEMENT METHOD

APPLIED TO ELECTROSTATIC

AXISYMMETRIC PROBLEMS

by

Dan V. Gibson

A thesis

presented to the School of Graduate Studies and Research

of the University of Ottawa

in partial fulfillment of the requirements

for the degree of

Master in Applied Science

in

Electrical Engineering



Dan V. Gibson, Ottawa, Canada, 1989

I hereby declare that I am the sole author of this document. I authorize the University of Ottawa to lend this thesis to other institutions or individuals for the purpose of scholarly research.

I further authorize the University of Ottawa to reproduce this thesis by photocopying or other means, in total or in part, at the request of other institutions or individuals for the purpose of scholarly research.

CONTENTS

ACKNOWLEDGEMENTS	viii
ABSTRACT	1
INTRODUCTION	3
THEORY	7
Geometry and boundary conditions	7
The Boundary Element Method	8
NUMERICAL PROCEDURE	18
Matrix Elements	18
Subregions	20
Computer implementation	23
Description of program	25
RESULTS	28
DISCUSSION AND CONCLUSIONS	37

APPENDIX A	39
APPENDIX B	41
APPENDIX C	45
APPENDIX D	48
REFERENCES	61

LIST OF FIGURES

Coaxial cable with protruded conductor	9
Geometrical elements of cylindrical symmetry	16
Division of contour into elements	18
Domain divided into two subregions	21
Distribution of field normal component inside external conductor	29
Capacitance of the system versus degree of filling	32
Coaxial cable configuration	35
Normalized capacitance versus frequency	36

LIST OF TABLES

Variation of system capacitance with four parameters . . .	30
Normalized Capacitance $Ct/\epsilon_0(b-a)$ of a 50- Ω air line and a 50- Ω teflon-dielectric line calculated analytically and by various methods including BEM	33
Comparison between potentials calculated analytically and by using BEM	34

ACKNOWLEDGEMENTS

To my supervisor, Dr. Michel Ney, many thanks for his time, continuous advice and guidance toward the completion of this thesis.

To Dr. George Costache, University of Ottawa and Dr. Cevdet Akyel, Ecole Polytechnique, Montréal, many thanks for their help in understanding many fine points related to this work.

To Dr. Jim Wight, Carleton University, special thanks for his comments and suggestions towards clarifying the contents and improving the appearance of this document.

To my colleagues, Mr. Andrew Douglas and Dr. Mike Goddard, many thanks for their help in drafting this manuscript and running the computer program.

To my wife Agneta, many thanks for her support and understanding.

ABSTRACT

An axisymmetric configuration consisting of a coaxial cable with a protruded middle conductor capable of hosting a variable degree of dielectric filling is studied. This structure may be used as a sensor for permittivity studies (e.g. in biological substances, time-domain reflectometry etc.). By means of optimizing the capacitance of the sensor, a method whereby a "smooth" matching between the impedance of the sensor and that of the sample is sought. The suitability of the Boundary Element Method to analyze this structure is assessed.

Radiation of energy and high-order propagation modes are neglected; the problem is quasi-static and the potential satisfies Laplace's equation.

A computer program which models the two-region configuration was developed. The program calculates the values of the potentials and fields along the conductors (and at internal points, if needed).

By varying configuration parameters: (i) internal aperture (distance between conductors inside the coaxial cable);

(ii) degree of filling the protruded cable with dielectric;
(iii) permittivities of the dielectric media both inside and outside the cable; (iv) length of protrusion, one determines the conditions under which the capacitance of the system is optimized.

The results reflect the expected behavior of the capacitance with configuration parameters. By applying the method to structures for which analytically-calculated values of the potential were known, it was found that the numerical results lay within 5% of the exact ones.

The study concludes that matching between sample and sensor is feasible and means to achieve such matching are developed. The Boundary Element Method is found to be a valuable tool in modelling and analyzing axisymmetrical configurations.

CHAPTER I

INTRODUCTION

A complete characterization of permittivity implies a large number of measurements over a wide range of frequencies. This is both time consuming and expensive. An alternative to the frequency-domain approach above, is to perform measurements in the time domain. In the latter case, a step pulse is used, containing all frequencies of interest. This method, known as time domain reflectometry (TDR), saves time and equipment.

The relation between the current through the sample, $I(x,t)$ and the voltage $V(x,t)$, modulated by the response function $\phi(t)$ is given by

$$I(t,x) = \frac{\partial}{\partial t} C_g \int_0^t dt' \phi(t-t') V(t',x) \quad (1)$$

where C_g is simply the geometric capacitance per unit length of line and $\phi(t)$ is the derivative of the response function to the step pulse $V(t)$.

The Laplace transform $\varphi(i\omega)$ of the response function $\phi(t)$ is related to the complex permittivity of the sample by

$\epsilon'(iw)=iw\phi(iw)$. It is apparent from the above discussion that the role of the capacitance is critical in the process of matching the sample cell to the transmission line ⁽¹⁵⁻²⁰⁾.

Dielectric properties determine the absorption and propagation of electromagnetic energy properties of materials. In this work an attempt is made to calculate the capacitance of a coaxial cable used as a sensor. The analysis is performed using the Boundary Element Method (BEM).

In the BEM, the external surface of a domain is divided into a series of elements in the same way as in Finite Element Method (FE). Over these elements, the functions under consideration vary according to predetermined rules.

C. A. Brebbia, was of the opinion⁽¹⁾ that because of the smaller system of equations, the reduction of data required to run a problem and its suitability for infinite domains, the BEM would offer an advantage over "domain"-type solutions such as FE. Like all approximate methods, BEM can be interpreted as a particular application of weighted residual techniques.

BEM is now being used in Electrical Engineering fields spanning the range from waveguides and dielectric resonators⁽²⁾ to RF circuit analysis computing⁽³⁾, from antenna patterns⁽⁴⁾ to eddy-currents distribution⁽⁵⁾.

Medical applications⁽⁶⁻⁹⁾ of microwave energies require a knowledge of the distribution of permittivity in tissue. For low frequencies, the sensor sensitivity to changes in sample permittivity is heavily dependent upon its capacitance. A small capacitance results in a high impedance of the sensor compared to that of the line, and this leads to uncertainty in permittivity measurements⁽¹⁵⁾.

For small sample thicknesses, it is imperative that the capacitance of the system be maximized. Varying configuration parameters enables the finding of the conditions under which the capacitance of the system is maximized.

Matching the sample to the rest of the network is critical for the accuracy of these measurements. A special configuration to achieve this was proposed by Prof. C. Akyel, Ecole Polytechnique, Montréal. It is hoped that this configuration will enable a controlled match between the sensor and the dielectric sample.

In this work an attempt is made to calculate the electric field distribution along the boundaries of the proposed configuration. The surface charge distribution on the conductors is determined and the capacitance of the system calculated. Finally, the geometrical parameters are varied in order to optimize the electrical properties of the sensor, such as its

capacitance.

The method employed consists basically in finding a solution to Laplace's equation. That solution only approximately satisfies a set of boundary conditions. The preceding concept is then applied to elements in which the boundary is discretized. The result is a system of linear equations which remains to be solved by regular algebraic methods. As a result, solving the partial differential equation, accompanied by boundary conditions, has been reduced to an algebraic problem.

To summarize, the purpose of this thesis is twofold:

(i) to evaluate the application of BEM to a complex axisymmetric structure; (ii) to calculate the capacitance of the structure and to determine what set of configuration parameters would optimize its electrical parameters.

To verify the program, the method was also applied to an open-ended coaxial cable, for which capacitance calculations have been already performed both analytically ^(21,22), by use of FE and the Method of Moments (MoM) ⁽²³⁾.

CHAPTER II

THEORY

2.1 Geometry and boundary conditions

Fig. 1 shows the geometry of the problem. Subregion I, inside the coaxial cable is bounded by conductors arbitrarily held at 0 and $1V$ respectively. A virtual boundary, perpendicular to the conductors, is placed at a variable distance " l " inside the cable. There, the electric field is assumed to be in the plane of the boundary, thus assuming a zero normal derivative on it. Finally, the interface between the two dielectric media constitutes the other end of subregion I.

Subregion II is bounded by the upper part of the outer conductor and part of the protruded middle conductor. This subregion is assumed to be closed at infinity along a line of the electric field. Consequently, the field has a zero normal derivative along that part of the boundary (Neumann boundary condition).

The values of the potentials are given on the two conductors and the values of the potential derivative (electric field) on the inner virtual boundary of subregion I. BEM

calculates the electric field on the conductors, the potential on the inner boundary and both potential and field on the interface between the two subregions.

The normal to the surface is chosen to point outward from the conductor. This is achieved by imposing the rule that when going along the boundary in a counter-clockwise direction, the normal lies on the left-hand side.

2.2 The Boundary Element Method

Let $u_0(x,y,z)$ be the electrostatic potential defined over the domain Ω and satisfying the Laplace's equation.

$$\nabla^2 u_0 = 0 \text{ in } \Omega \quad (1)$$

with boundary conditions on Γ of the following two types:

$$u_0 = \bar{u} \quad (2)$$

$$q_0 = \frac{du_0}{dn} = \bar{q} \quad (3)$$

The reason our solution satisfies Laplace's equation as opposed to Helmholtz' is that we make the following assumption to simplify the problem: over the frequency range of interest, the radiation of energy and the higher-order propagation modes are neglected. This is the quasi-static assumption⁽¹⁴⁾.

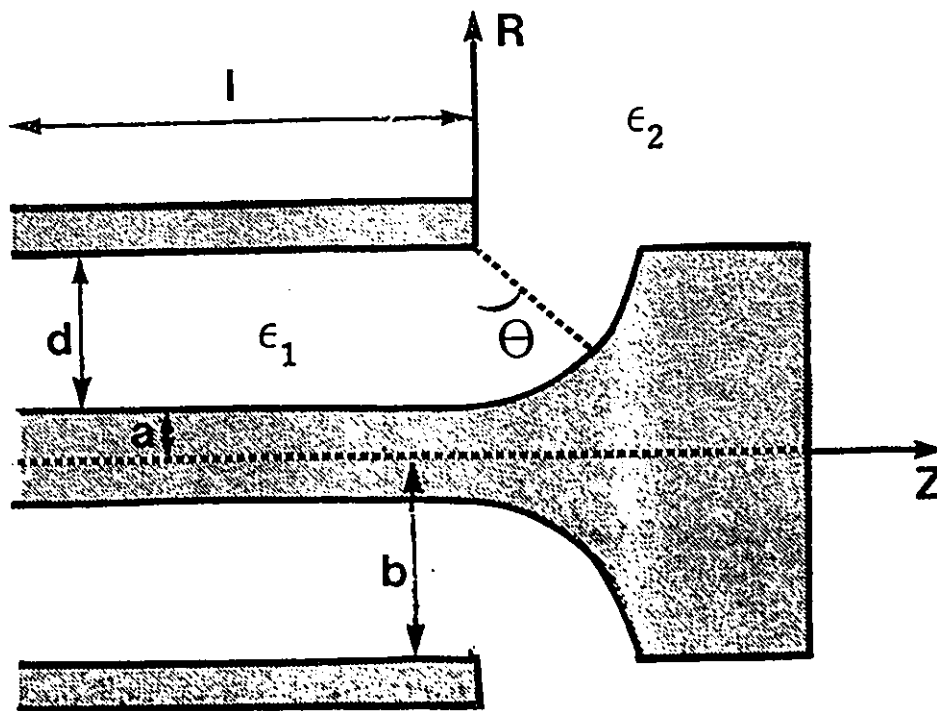


Figure 1: Coaxial cable with protruded conductor

Approximate numerical methods generate solutions, u , that differ from the exact one, u_0 . A set of linearly independent functions $\theta(x)$ is defined such that

$$u = \sum_{k=1}^N \alpha_k \theta_k + \alpha_0 \quad (4)$$

If we define the error functions:

$$R = \nabla^2 u \text{ in } \Omega \quad (5)$$

$$R_1 = u - \bar{u} \text{ on } \Gamma_1 \text{ and} \quad (6)$$

$$R_2 = q - \bar{q} \text{ on } \Gamma_2, \quad (7)$$

where Γ_1 and Γ_2 are parts of the total boundary Γ ($\Gamma = \Gamma_1 + \Gamma_2$). These errors are distributed in such a way that they be zero in an average sense. Another set of linearly independent functions $\phi(x)$ and a weighting function w are defined, that satisfy:

$$w = \sum_{k=1}^N \beta_k \phi_k \quad (8)$$

where β_k , $k = 1, n$, are constants.

Various approaches to finding the solution are now possible, depending on the conditions we impose on the expressions above (4-8). A comparison between the Boundary Element Method and the Method of Moments⁽²⁴⁾ is detailed here.

Both methods solve a deterministic problem. The approximate solution satisfies certain boundary conditions. The original differential equation (say Laplace's equation) is reduced to a set of linear algebraic equations.

In MOM the approximate functions are sought to satisfy the boundary conditions (or some of them) and be approximate in the domain. In BEM, the functions satisfy the governing equation in the domain and only approximately satisfy the boundary conditions. In MOM it is customary for the weighting functions to be Dirac functions (point matching) and pulse functions for basis (subsection method). In BEM the weighting function is usually chosen to be the fundamental solution of the governing equation

in that space. Volume integrals are accordingly eliminated.

The BEM imposes the following conditions:

a) u and w both satisfy the governing equation:

$$\nabla^2 u = 0$$

$$\nabla^2 w = 0$$

b) u only approximately satisfies the boundary conditions (2) and (3)

$$u = \bar{u} \text{ on } \Gamma_1 \text{ and}$$

$$q = \bar{q} \text{ on } \Gamma_1$$

We define the inner product

$$\langle R, w \rangle = \int_{\Omega} R w \, d\Omega \quad (9)$$

where R is an error function as defined in (5) and w is the weighting function defined in (8). The inner product above is the mathematical representation of the idea of distributing the error over a domain. It can be shown (Appendix A) that

$$\int_{\Omega} R w \, d\Omega = \int_{\Gamma_2} R_2 w \, d\Gamma - \int_{\Gamma_1} R_1 w \, d\Gamma \quad (10)$$

From Appendix A (c) we obtain:

$$\int_{\Omega} \nabla^2 w \, u \, d\Omega = - \int_{\Gamma} q \, w \, d\Gamma + \int_{\Gamma} u \frac{dw}{dn} \, d\Gamma$$

assuming w to be the fundamental solution to Laplace's equation

$$\nabla^2 w = -\delta(r-r')$$

the following equation is obtained with the notation change $w \equiv u^*$ ($dw/dn = q^*$):

$$c(\mu) u(\mu) + \int_{\Gamma} u(x) q^*(\mu, x) \, d\Gamma(x) = \int_{\Gamma} q(x) u^*(\mu, x) \, d\Gamma(x) \quad (11)$$

where μ are the coordinates of the source and x those of the point of interest.

For a smooth boundary, it can be shown that $c(\mu)$ is $\frac{1}{2}$.

For a boundary that is not smooth, a means to avoid the calculation of $c(\mu)$ will be shown later.

To reduce equation (11) to a suitable algebraic form to be solved by a numerical approach, the following general steps are taken⁽²⁵⁾.

(a) The boundary Γ is discretized into a series of elements over which the potential and its normal derivative are assumed to vary according to interpolation functions (4). The geometry of these segments can be modelled using straight lines, circular arcs etc.

In this work straight lines are used.

(b) By using the method of collocation, the discretized equation is applied to a number of particular nodes within each element.

(c) Integrals over each element are carried out either analytically or using a numerical quadrature (e.g. four-point Gaussian quadrature).

(d) The boundary conditions are imposed along each element: either the potential or its derivative is given, and a system of linear equations is obtained. The solution of the system of equations provides the remaining unknowns (either potentials or their derivatives).

Using (11), the values of the potential can be calculated at any internal point ($c(\mu)=1$).

The particular configuration of Figure 1 has the following characteristics that have to be addressed separately.

(a) The geometry and the boundary conditions are axisymmetrical;

(b) The geometry consists of two separate and distinct subregions;

(c) One of the subregions has finite boundaries, the other has boundaries at infinity;

(d) The two subregions are connected by an internal boundary or interface. On this interface, neither the potential nor its derivative is known. Two extra conditions will enable one to solve the final system of equations, which would otherwise have more unknowns than equations. The four points (a) to (d) are addressed below.

(a) The three-dimensional fundamental solution of Laplace's equation is written in cylindrical polar coordinates (Fig. 2):

$$u^* = \frac{1}{4\pi} \frac{1}{r(\mu, x)} = \frac{1}{4\pi [R'^2 + R^2 - 2R'R \cos(\theta' - \theta) + (Z' - Z)^2]^{\frac{1}{2}}}$$

and the axisymmetric potential can be calculated as follows:

$$\bar{u}^* = \int_0^{2\pi} u^* d\theta = \frac{K(m)}{\pi (a+b)^{\frac{1}{2}}} \quad (12)$$

where

$$a = R'^2 + R^2 + (Z' - Z)^2$$

$$b = 2R'R$$

$$m = \frac{2b}{a+b}$$

The normal derivative of the fundamental solution along the boundary contour $\bar{\Gamma}$ is given by:

$$\bar{q}' = \frac{1}{\pi (a+b)^{1/2}} \left\{ \frac{1}{2R} \left[\frac{R'^2 - R^2 + (Z'-Z)^2}{a-b} E(m) - K(m) \right] n_r + \right. \\ \left. + \frac{Z'-Z}{a-b} E(m) n_z \right\} \quad (13)$$

where n_r and n_z are the direction cosines of the normal to the surface Γ and $K(m)$ and $E(m)$ are the complete elliptic integrals of the first and second kinds.

The bar on \bar{u}' and \bar{q}' indicates the cylindrical solution. The derivation of expressions (12) and (13) is given in Appendix B.

The element of surface $d\bar{\Gamma}$ can be written for cylindrical symmetry:

$$d\bar{\Gamma} = R d\theta d\bar{r}$$

$\bar{\Gamma}$ is the generating boundary contour which is the intersection of Γ with the R^*-Z semiplane (Fig. 2).

(b) For each subregion, and assuming that the potential or its normal derivative is constant over each element, the fundamental equation (11) is transformed as follows:

$$c u + \int_{\Gamma} u \left[\int_{\bar{\Gamma}} q' d\theta \right] R d\bar{\Gamma} = \int_{\Gamma} q \left[\int_{\bar{\Gamma}} u' d\theta \right] R d\bar{\Gamma} \quad (14)$$

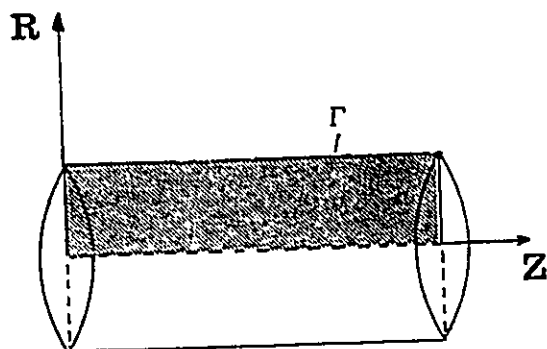


Figure 2: Geometrical elements of cylindrical symmetry

The square brackets are \bar{u}' and \bar{q}' calculated above in (12) and (13), so the final expression is:

$$c u + \int_r u \bar{q}' R d\Gamma = \int_r q \bar{u}' R d\Gamma \quad (15)$$

Expression (15) is discretized and the values of the integrals are calculated over each element forming the boundary. Calculations are performed for each subregion separately.

(c) Equation (11) applies to infinite regions if a certain regularity condition is fulfilled by the potential and its derivative at infinity. The condition is:

$$\lim_{R \rightarrow \infty} \int (q u' - u q') d\Gamma = 0 \quad (16)$$

It will be shown later that the regularity condition is violated under certain conditions relevant to the solution of our problem.

(d) The interface between two subregions is formally considered as part of each subregion separately. The link between the values of the potential and its derivative in the two subregions is provided by the following conditions:

$$U_1^I = U_2^I \quad (17)$$

$$\epsilon_1 Q_1^I = \epsilon_2 Q_2^I \quad (18)$$

where the upperscript implies the internal boundary or interface and ϵ_1 and ϵ_2 are the permittivities of the two subregions. The second condition (18) is the continuity condition for the normal component of the electrical displacement at the interface between two dielectric media.

CHAPTER III

NUMERICAL PROCEDURE

3.1 Matrix Elements

To discretize the problem we divide the boundary in a series of segments or boundary elements (Fig. 3). The points where the values of the potential and of the electrical field are considered are at the middle of each segment and those values are assumed to be constant along each element.

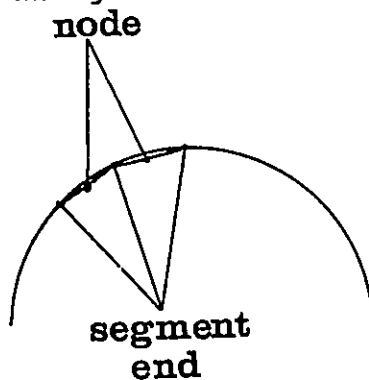


Figure 3: Division of contour into elements

The boundary is discretized into N elements of which N_1 are assumed to belong to Γ_1 and N_2 to Γ_2 . For each such element either the potential u or its derivative q is known. These known values are constant over the element and accordingly can be taken out of the integral in (15). Equation (15) can be discretized as follows:

$$c_1 u_1 + \sum_{j=1}^N \left(\int_{r_j} \bar{q}^* R d\bar{\Gamma} \right) u_j = \sum_{j=1}^N \left(\int_{r_j} \bar{u}^* R d\bar{\Gamma} \right) q_j \quad (19)$$

where \bar{u}^* and \bar{q}^* are given by (12) and (13).

The integrals of the type $\int_{r_j} \bar{q}^* R d\bar{\Gamma}$, denoted H_{ij} , relate the middle of segment "i", whose coordinates are R' and Z' in (13), to the element "j", over which the integral is carried out.

Similarly, integrals of the type $\int_{r_j} \bar{u}^* R d\bar{\Gamma}$ are denoted

G_{ij} and we have:

$$c_1 u_1 + \sum_{j=1}^N H_{ij} u_j = \sum_{j=1}^N G_{ij} q_j \quad (20)$$

Equation (20) is written for each segment "i" and for each subregion. The expressions obtained in this thesis for the matrix elements of G and H are valid for any axisymmetrical configuration whose boundaries are divided into constant elements.

For a finite subregion and a smooth boundary $c_1 = \frac{1}{2}$ and we define:

$$H_{ij} = \begin{cases} H_{ij} & i \neq j \\ H_{ij} + \frac{1}{2} & i = j \end{cases} \quad (21)$$

and (20) can be written:

$$\sum_{j=1}^N H_{ij} u_j = \sum_{j=1}^N G_{ij} q_j \quad ; \quad i = 1, 2, \dots, N \quad (22)$$

or in matrix form:

$$H U = G Q \quad (23)$$

The above approach is applied to each of the two subregions.

3.2 Subregions

Figure 4 shows the general aspect of a configuration with two subregions. The boundary of each contains the regular segments (over which we know either u or its derivative q) and the internal boundary or interface (over which we know neither).

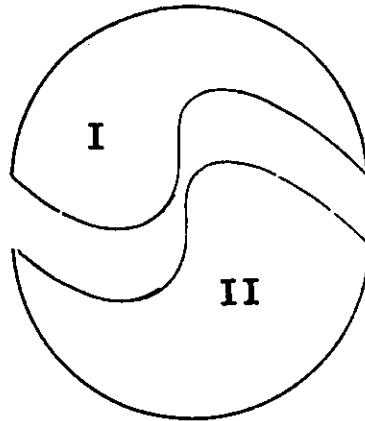


Figure 4: Domain divided into two subregions

Each matrix H or G , for each of the two subregions, has two bands: one that refers to the regular boundary and one that refers to the interface. They are denoted H_1 , H_2 , G_1 and G_2 , and H_1^I , H_2^I , G_1^I and G_2^I respectively.

Also the potentials and their derivatives correspond to values on the regular boundary, U_1 , U_2 , Q_1 , Q_2 , or on the interface, U_1^I , U_2^I , Q_1^I , Q_2^I .

For each subregion a matrix equation similar to (23) can be written:

$$\begin{bmatrix} H_1 & H_2^I \end{bmatrix} \begin{vmatrix} U_1 \\ U_1^I \end{vmatrix} = \begin{bmatrix} G_1 & G_2^I \end{bmatrix} \begin{vmatrix} Q_1 \\ Q_1^I \end{vmatrix} \quad (24)$$

and

$$\begin{bmatrix} H_2 & H_2^I \end{bmatrix} \begin{vmatrix} U_2 \\ U_2^I \end{vmatrix} = \begin{bmatrix} G_2 & G_2^I \end{bmatrix} \begin{vmatrix} Q_2 \\ Q_2^I \end{vmatrix} \quad (25)$$

Taking into account the compatibility conditions on the interface (17) and (18), we can combine (24) and (25) into:

$$\begin{vmatrix} H_1 & H_1^I & 0 \\ 0 & H_2^I & H_2 \end{vmatrix} \begin{vmatrix} U_1 \\ U_1^I \\ U_2 \end{vmatrix} = \begin{vmatrix} G_1 & G_1^I & 0 \\ 0 & \frac{\epsilon_1}{\epsilon_2} G_2^I & G_2 \end{vmatrix} \begin{vmatrix} Q_1 \\ Q_1^I \\ Q_2 \end{vmatrix} \quad (26)$$

or

$$\begin{vmatrix} H_1 & H_1^I & 0 & -G_1^I \\ 0 & H_2^I & H_2 & \frac{\epsilon_1}{\epsilon_2} G_2^I \end{vmatrix} \begin{vmatrix} U_1 \\ U_1^I \\ U_2 \\ Q_1^I \end{vmatrix} = \begin{vmatrix} G_1 & 0 \\ 0 & G_2 \end{vmatrix} \begin{vmatrix} Q_1 \\ Q_2 \end{vmatrix} \quad (27)$$

In fact, the system (27) can be directly assembled so that all the unknowns are on the left side in X and the known values in F , to give a system of the following form:

$$A X = F \quad (28)$$

3.3 Computer implementation

The off-diagonal elements of G and H are calculated using a four-point Gaussian quadrature⁽²⁶⁾. The diagonal elements however contain singularities and are better calculated analytically.

To this end \bar{u}^* and \bar{q}^* are written in terms of Legendre functions of the second kind:

$$\bar{u}^* = \frac{8^{\frac{1}{2}} Q_{-1}(\tau)}{b^{\frac{1}{2}}} \quad (29)$$

$$\begin{aligned} \bar{q}^* = - \frac{8^{\frac{1}{2}}}{R b^{\frac{1}{2}}} \left\{ \left[\frac{Q_{-1}(\tau)}{2} + \frac{R'^2 - R^2 + (Z' - Z)^2}{b} \frac{dQ_{-1}(\tau)}{d\tau} \right] n_R + \right. \\ \left. + \frac{(Z' - Z)}{R'} \frac{dQ_{-1}(\tau)}{d\tau} n_z \right\} \quad (30) \end{aligned}$$

$$\text{where } \tau = 1 + \frac{a - b}{b} \quad (31)$$

For small values of τ , the Legendre function $Q_{-1}(\tau)$ and its derivative can be approximated as follows:

$$Q_{-1}(\tau) = - \frac{1}{2} \ln \left(\frac{\tau - 1}{32} \right) \quad (32)$$

$$\frac{dQ_{-1}(\tau)}{d\tau} = - \frac{1}{2(\tau-1)} \quad (33)$$

Elements G_{ii} are calculated in Appendix C using the above formulas (29-33).

For finite regions, as already mentioned, the coefficient c_i in equation (20) is $\frac{1}{2}$. For boundaries that are not smooth a means to calculate H_{ii} (21) without calculating c_i is presented below:

- assuming a uniform potential is applied over the entire boundary, the normal derivative (q) must be zero, and equation (23) becomes:

$$H U = 0 \quad (35)$$

This means that the sum of all the elements of H in a row ought to be zero and the value of the diagonal element is simply:

$$H_{ii} = - \sum_{\substack{j=1 \\ j \neq i}}^N H_{ij} \quad (36)$$

For infinite regions however, where the regularity condition (16) is not satisfied, equation (36) should be amended. In our case:

$$\lim_{R \rightarrow \infty} \int_{\Gamma} q^* d\Gamma = -1 \quad (37)$$

so for the region with infinite boundaries, the diagonal elements of H are calculated according to the formula:

$$H_{ii} = - \sum_{\substack{j=1 \\ j \neq i}}^N H_{ij} + 1 \quad (38)$$

3.4 Description of the program

The program has six main parts:

1. (a) input of initial parameters
 (b) discretizing the boundaries of the two subregions, by dividing them into linear segments;
2. (a) calculating the off-diagonal elements of G and H (subroutine INTE);
 (b) calculating the diagonal elements of G (subroutine INLO);

- (c) calculating the diagonal elements of H by using (36) and (38);
3. (a) forming the large matrix on the left side of (27)
 - (b) solving the system of equations (28)(subroutine SLNPD);
 4. (a) rearranging and identifying the results of 3(b) above (which unknown is potential and which its derivative)
 - (b) calculating the potential at chosen internal points, if needed;
 - (c) calculating the capacitance of the system (subroutine INTER);
 5. calculating elliptic integrals of the first and second kinds⁽²⁷⁾, $K(m)$ and $E(m)$.
 6. outputting the results (subroutine OUTPT).

The number of segments in each subregion is variable. The circular part of the protrusion is divided into 10 elements. The interface between the two media can be moved freely, in such a way as to form an angle between 0 and 90 degrees with the end of the coaxial cable.

The program requests the input of an angle and as a

consequence, it divides the ten elements of the circular part between the two subregions. The fixed number of elements in each subregion are 22 in the first and 16 in the second. To each, according to the position of the interface, up to ten elements are added.

Subregion I is bounded, while subregion II is not. The latter is supposed to be closed at infinity along an electric field line. Along this line there are of course no elements.

The listing of the program is given in Appendix D.

CHAPTER IV

RESULTS

The program determines the unknown values of the potential and of the electrical field in both regions, at the middle of each segment and on the interface. The length of cable taken into account is five times its internal aperture. It was assumed, based on previous studies, that this length would ensure electric field lines normal to the conductors. The results provide a particularly-smooth picture of the field along the conductors. Figure 5 shows the values of the electric field on the inside of the external conductor.

At sharp geometrical discontinuities, like edges, the computed values show continuous behavior. At the virtual boundary inside the coaxial cable, the values obtained do not show any discontinuity. Such a discontinuity may be expected due to the fact that points close to that boundary have neighboring segments only on one side. The application of the method of images, which in similar cases is used to alleviate the problem, is not necessary in this case. This saves considerable memory space and CPU time, because the doubling of the number of unknowns is avoided.

Using the proportionality between the electric field

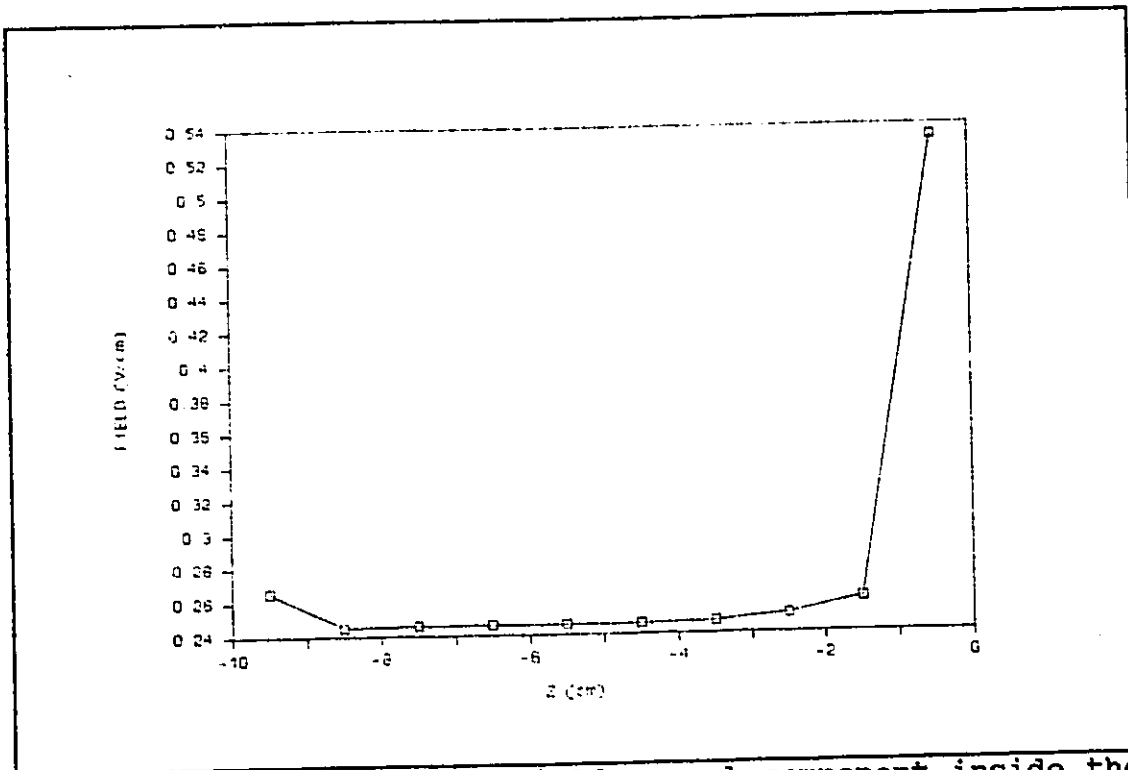


Figure 5: Distribution of field normal component inside the external conductor

and the surface charge on the conductors,

$$\sigma = \epsilon E_n$$

the total charge on one of the conductors and therefrom the capacitance of the system are calculated.

Four parameters: (i) the permittivity inside the cable, (ii) the angle between the dielectric interface and the end plane of the cable, (iii) the internal aperture of the cable and (iv) the length of the protruded part, are varied and the capacitance of the system is calculated for different

combinations. The results are shown in Table 1. Examination of Table 1 reveals that the capacitance increases with increased permittivity inside the cable and decreases with internal aperture. The more the circular part in Fig. 1 is filled with dielectric, the larger the capacitance. The length of the protruded part does not influence the capacitance.

Varying the degree of filling the protruded part with dielectric provides a particularly smooth choice of the capacitance for purposes of matching the sensor to the rest of the line. Figure 6 shows the behavior of the capacitance versus the degree of filling.

TABLE 1

Variation of system capacitance with four parameters:

ϵ_1 - permittivity inside cable

d - internal aperture radius

t - Z-coordinate (length) of protruded part

θ - degree of filling the protruded part with dielectric

ϵ_1	d	t	θ	C
			5	90.14
1.5	2.0	3.5	40	90.96
			85	92.44

			5	104.56
2.0	2.0	3.5	40	106.14
			85	108.54

			5	118.95
2.5	2.0	3.5	40	121.32
			85	124.58

			5	119.67
2.5	1.8	3.5	40	122.99
			85	127.68

			5	122.45
2.5	1.6	3.5	40	126.70
			85	131.96

			5	127.36
2.5	1.4	3.5	40	132.33
			85	137.82

			5	134.74
2.5	1.2	3.5	40	140.36
			85	146.00

			5	145.63
2.5	1.0	3.5	40	151.95

			85	157.80
			5	145.56
2.5	1.0	2.8	40	151.88
			85	157.75
			5	145.69
2.5	1.0	4.2	40	151.99
			85	157.84

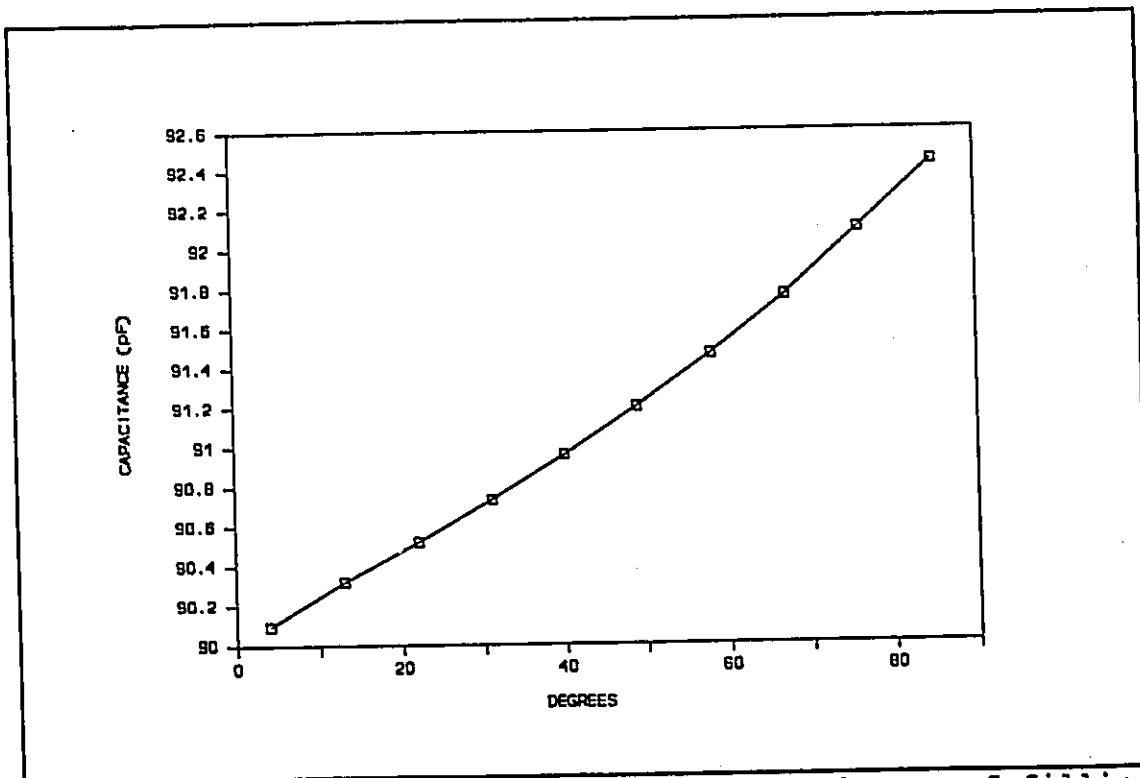


Figure 6: Capacitance of the system versus degree of filling

The same basic program was applied to two different configurations: a coaxial 50- Ω air line and a 50- Ω teflon-dielectric line. The values of the ratio b/a are 2.303 and 3.268 respectively. According to the formula^(21,22):

$$C_r = \frac{2 \epsilon_0}{k \ln^2(b/a)} \int [2 \text{Si}(k(a^2+b^2-2ab\cos\theta)^{1/2}) - \text{Si}(2ka\sin\frac{1}{2}\theta) - \text{Si}(2kb\sin\frac{1}{2}\theta)] d\theta$$

where $\text{Si}(x)$ is the sine integral function, $k=2\pi/\lambda$, λ is the wavelength and ϵ_0 is the free-space permittivity, the values of the normalized capacitance is calculated and the results are shown in Fig. 8.

The values of the normalized capacitance obtained by the application of the boundary element method are given in Table 2. They are close to the values obtained analytically and by using other numerical methods for the same ratios b/a .

TABLE 2

Normalized Capacitance $C_t/\epsilon_0(b-a)$ of a 50- Ω air line and a 50- Ω teflon-dielectric line calculated analytically and by various methods including BEM

Analytical	FEM	MOM	BEM
4.295	4.311	4.066	4.352
2.5	2.481	2.383	2.589

The results obtained are in good agreement with theoretical calculations for the potential and indicate that the method is quite accurate. Values of the potential calculated analytically are compared with obtained by using BEM. These values are computed at a distance "l" inside the cable, given by the condition $l=5d$, where "d" is the spacing between the two conductors. At those locations the effect of distortions due to field non-homogeneities is negligible. The analytical formula for the potential can therefore be used: $V(r) = \ln(r/a)/\ln(b/a)$. A comparison is given in Table 3.

TABLE 3

Comparison between potentials calculated analytically and by
using BEM

Analytical	BEM	error %
0.683	0.684	0.15
0.861	0.868	0.81
0.431	0.424	1.6
0.341	0.341	0.01
0.817	0.826	1.08
0.338	0.324	4.14
0.839	0.850	1.30
0.379	0.359	5.35
0.2399	0.2397	0.01

In terms of programming, the number of segments can be increased at will, computer memory permitting. A typical running time for 68 unknowns (potential or electrical field) was 22 seconds. For the same configuration, the Finite Element Method took 5 seconds and the Moment Method 80⁽²³⁾.

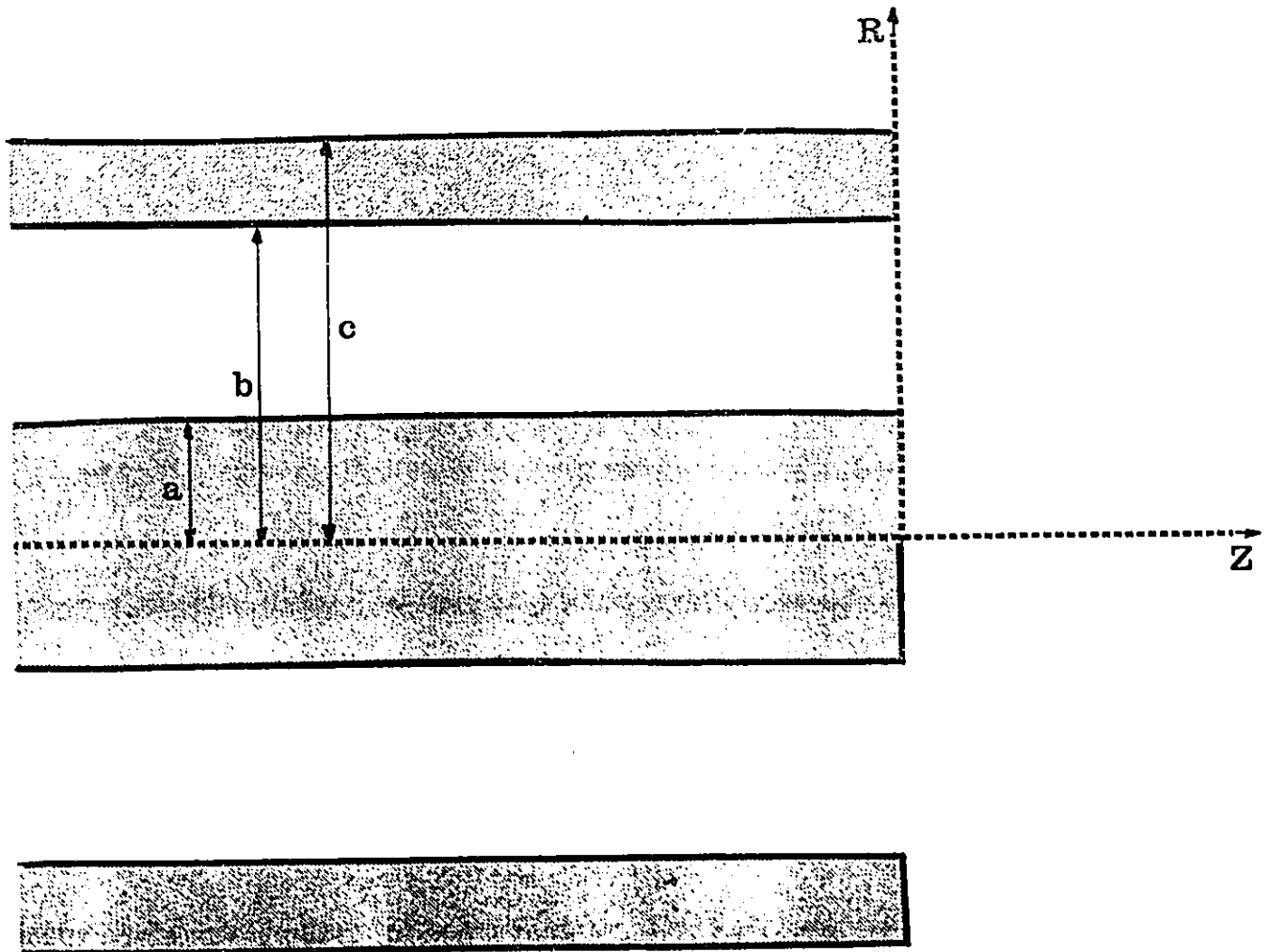


Figure 7: Coaxial cable configuration

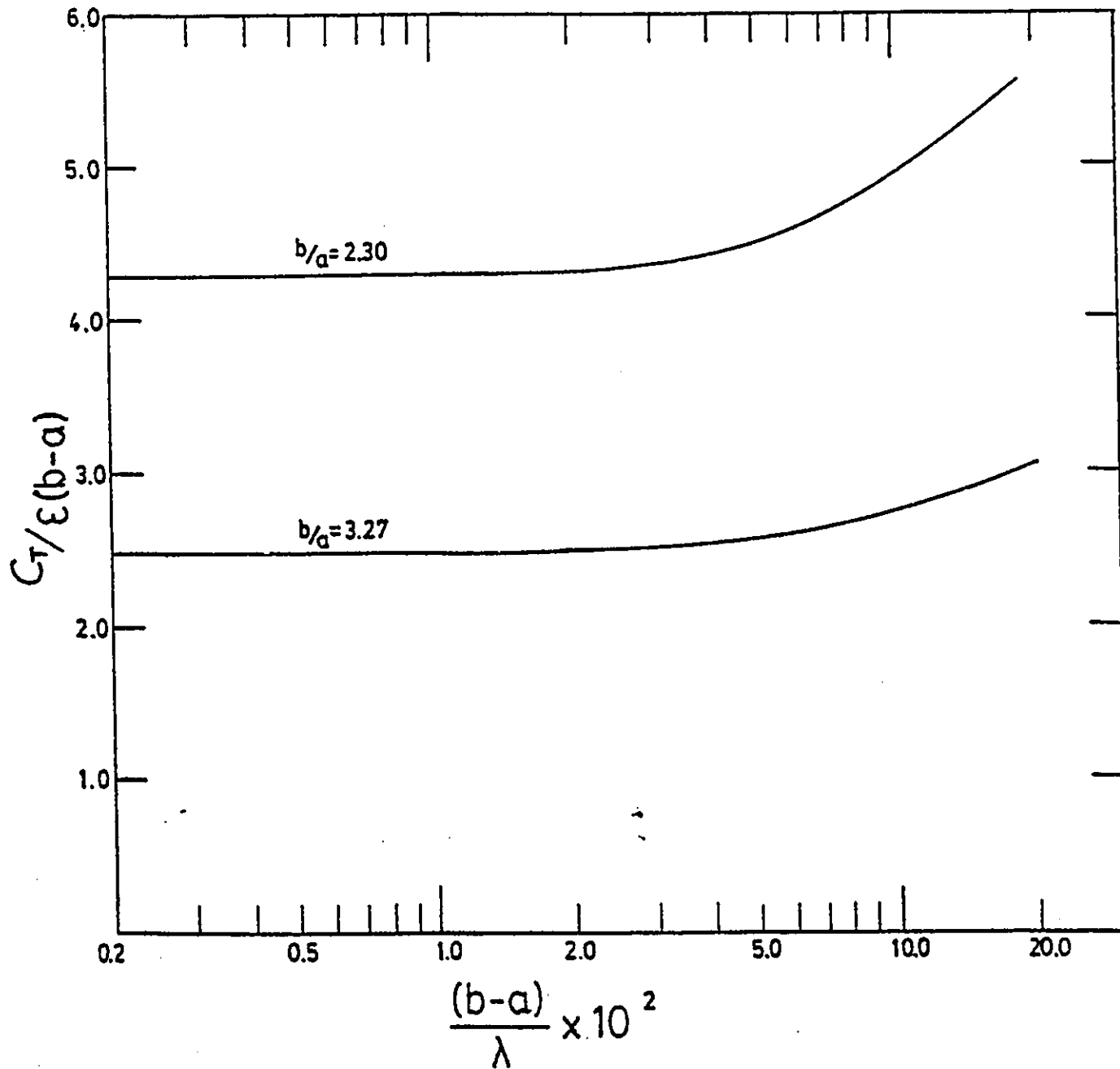


Figure 8: Normalized capacitance versus frequency
for a coaxial cable⁽²³⁾

CHAPTER V

DISCUSSION AND CONCLUSIONS

In this work, the application of BEM to a two-region, axisymmetric, unbounded structure, was evaluated. The potential and its derivative (electric field) were computed on the boundary and therefrom the charge distribution and the capacitance of the system were calculated. Four parameters were varied in order to determine what geometry and materials (internal dielectric permittivity) would best be suited to maximize the capacitance. The larger the capacitance, the better the use of the system as a permittivity sensor. The parameters were:

- the permittivity of the dielectric inside the cable;
- the internal aperture of the cable;
- the degree of filling the protruded part with dielectric material and
- the length of the protruded part of the inner conductor.

The method used to calculate the potential and electric field on the conductors was to discretize the boundaries into a series of segments and to apply a weighted residual expression on each of them. On each segment either the potential or the electric field was known. For each of the two subregions of our configuration, a set of linear equations was obtained. Together

with compatibility conditions on the interface between the two subregions, a large matrix equation was obtained. Its solution would give the remaining unknowns.

With additional sets of a) compatibility conditions (17) and (18), b) arrays containing the coordinates of segment ends and c) larger matrices of the type (27) and (28), the computer program could be expanded to configurations consisting of more than two subregions.

It was found that a maximum capacitance would be encountered when the dielectric permittivity is large and the dielectric occupies a large space within the cavity of the protruded part. Also, as it was expected, the smaller the inner aperture, the larger the capacitance. The length of the protruded part of the inner conductor does not influence the capacitance.

Based on the comparisons made with other numerical and analytical methods, BEM appears to be a valuable tool in computing capacitance values. BEM deals with linear segments for an axisymmetric problem, while FEM uses triangles. Input of data appears to be simpler in BEM. BEM is easily adaptable to new configurations due to the fact that only end points of each segment are inputted. Also, the solutions for fields and potentials do not display any unwanted discontinuities; in most cases the method of images is avoided.

APPENDIX A

Generalized weighted residual expression

From the weighted residual expression:

$$\int_{\Omega} \nabla^2 u w \, d\Omega = 0 \quad (a)$$

Integrating by parts:

$$\int_{\Omega} \frac{du}{dx_k} \frac{dw}{dx_k} \, d\Omega = \int_{\Gamma} q w \, d\Gamma, \quad \text{where } q = \frac{du}{dn} \quad (b)$$

and integrating again,

$$\int_{\Omega} \nabla^2 w u \, d\Omega = \int_{\Gamma} u \frac{dw}{dn} \, d\Gamma - \int_{\Gamma} q w \, d\Gamma \quad (c)$$

Introducing the boundary conditions,

$$u = \bar{u} \quad \text{on } \Gamma_1 \text{ and}$$

$$q = \bar{q} \quad \text{on } \Gamma_2,$$

(c) becomes:

$$\int_{\Omega} \nabla^2 w u \, d\Omega = \int_{\Gamma_1} u \frac{dw}{dn} \, d\Gamma + \int_{\Gamma_2} u \frac{dw}{dn} \, d\Gamma - \int_{\Gamma_1} q w \, d\Gamma - \int_{\Gamma_2} q w \, d\Gamma \quad (e)$$

To demonstrate that we make an approximation when imposing the boundary conditions above, we integrate twice by parts (e) to

retrieve the operator $\nabla^2 u$ and obtain:

$$\int_{\Omega} \nabla^2 u w \, d\Omega = \int_{\Gamma_2} (q - \bar{q}) w \, d\Gamma - \int_{\Gamma_1} (u - \bar{u}) \frac{dw}{dn} \, d\Gamma \quad \text{or} \quad (f)$$

$$\int_{\Omega} R w \, d\Omega = \int_{\Gamma_2} R_2 w \, d\Gamma - \int_{\Gamma_1} R_1 \frac{dw}{dn} \, d\Gamma \quad (g)$$

APPENDIX B

Derivation of axisymmetric fundamental solution of Laplace's equation and its normal derivative

The three-dimensional solution of Laplace's equation

$$\nabla^2 u^*(\mu, x) = 0 \quad (a)$$

is (making abstraction of the factor $1/4\pi$):

$$\begin{aligned} u^*(\mu, x) &= 1/r(\mu, x) = \\ &= 1/ \{R^2(x)+R^2(\mu)-2R(x)R(\mu)\cos[\theta(\mu)-\theta(x)]+[Z(x)-Z(\mu)]^2\}^{1/2} \end{aligned} \quad (b)$$

The axisymmetrical solution is:

$$\bar{u}^* = \int_0^{2\pi} u^*(\mu, x) d\theta(x) \quad (c)$$

Notation:

$$R(\mu) = R'; \quad Z(\mu) = Z'; \quad \theta(\mu) = \theta'$$

$$R(x) = R; \quad Z(x) = Z; \quad \theta(x) = \theta$$

$$a = R'^2 + R^2 + (Z' - Z)^2$$

$$b = 2RR'$$

$$m = 2b/(a+b)$$

$$\bar{u}^* = \frac{1}{(a+b)^{1/2}} \int_0^{2\pi} \frac{d\theta}{\left[1 - \frac{b}{(a+b)} (1 + \cos(\theta' - \theta))\right]^{1/2}} \quad (d)$$

After simple mathematical manipulations and applying basic properties as:

$$\int_{-x}^{x-\pi} f(\alpha) d\alpha = \int_0^{\pi} f(\alpha) d\alpha \quad \text{for } f(\alpha) = f(\alpha + \pi) \text{ and}$$

$$\int_{-y}^y f(x) dx = 2 \int_0^y f(x) dx \quad \text{for } f(x) = f(-x)$$

we obtain

$$\bar{u}^* = \frac{K(m)}{(a+b)^{1/2}} \quad \text{where} \quad (e)$$

$$K(m) = \int_0^{\pi/2} [1 - m \sin^2(\theta)]^{-1/2} d\theta$$

For the derivative \bar{q}^* we have:

$$\bar{q}^*(R, Z) = \frac{d}{dn} [\bar{u}^*(R, Z)] \quad \text{or}$$

$$\bar{q}^* = \frac{d}{dR} (\bar{u}^*) \frac{dR}{dn} + \frac{d}{dZ} (\bar{u}^*) \frac{dZ}{dn}$$

$$\frac{d}{dR} [(a+b)^{-1} K(m)] = K(m) \frac{d}{dR} [(a+b)^{-1}] + (a+b)^{-1} \frac{d}{dm} [K(m)] \frac{dm}{dR}$$

and similarly for d/dZ . The calculations are simple and only one of the above derivatives is presented below:

$$\begin{aligned} \frac{d}{dm} [K(m)] &= \frac{d}{dm} \int_0^{\pi/2} \frac{dx}{(1-m\sin^2 x)^{1/2}} = \frac{1}{2} \int_0^{\pi/2} \frac{\sin^2 x \, dx}{(1-m\sin^2 x)^{3/2}} = \\ &= \frac{1}{2m} \left[\int_0^{\pi/2} \frac{dx}{(1-m\sin^2 x)^{3/2}} - K(m) \right] \end{aligned} \quad (e)$$

To express the integral in (e) in terms of elliptic integrals of the first and second kinds, the following mathematical subtlety⁽²⁸⁾ is used:

$$\frac{d}{d\theta} \left[\frac{\sin\theta \cos\theta}{(1-m\sin^2 x)^{1/2}} \right] = \frac{1-2\sin^2\theta+m\sin^4\theta}{(1-m\sin^2 x)^{3/2}}$$

or

$$m \frac{d}{d\theta} \left[\frac{\sin\theta \cos\theta}{(1-m\sin^2x)^{\frac{1}{2}}} \right] = (1-m\sin^2x)^{\frac{1}{2}} - (1-m) \frac{1}{(1-m\sin^2x)^{\frac{3}{2}}}$$

and by integration,

$$m \int_0^{1/2\pi} \frac{d}{d\theta} \left[\frac{\sin\theta \cos\theta}{(1-m\sin^2x)^{\frac{1}{2}}} \right] d\theta = E(m) - (1-m) \int_0^{1/2\pi} \frac{d\theta}{(1-m\sin^2x)^{\frac{3}{2}}}$$

The left-hand side intergral is zero and we have:

$$\int_0^{1/2\pi} \frac{d\theta}{(1-m\sin^2x)^{\frac{3}{2}}} = \frac{1}{1-m} E(m) \quad (f)$$

Introducing (f) in (e) and after performing the derivatives, we obtain:

$$\bar{q}^2 = \frac{1}{\pi (a+b)^{\frac{1}{2}}} \left\{ \frac{1}{2R} \left[\frac{R'^2 - R^2 + (Z'-Z)^2}{a-b} E(m) - K(m) \right] n_R + \right. \\ \left. + \frac{Z'-Z}{a-b} E(m) n_R \right\}$$

APPENDIX C

From the expression of the potential in terms of Legendre functions of the second kind⁽²⁵⁾:

$$\bar{u}^* = \frac{8^{\frac{1}{2}} Q_{-1}(\tau)}{b^{\frac{1}{2}}} \quad (a)$$

For small values of τ ($\tau = 1 + \frac{a-b}{b}$) we have the following approximation:

$$Q_{-1}(\tau) = -\frac{1}{2} \ln \left(\frac{\tau-1}{32} \right) \quad (b)$$

We have to calculate G_{11} , the diagonal elements of G . Their expression is:

$$G_{11} = \int_{r_1} \bar{u}^* R \, d\Gamma \quad (c)$$

From (a), (b) and (c) we have the expression:

$$G_{11} = - \int_{r_1} \ln \left[\frac{(R-R')^2 + (Z-Z')^2}{64 R R'} \right] \left(\frac{R}{R'} \right)^{\frac{1}{2}} d\Gamma \quad (d)$$

after a few simple changes of variable, we obtain the following

expression for (d):

$$G_{11} = -\frac{L}{2} \left[\ln\left(\frac{L^2}{256R'^2}\right) I_1 + I_2 - I_3 \right]$$

where L is the length of segment "i" along which we perform the integration and I_1 , I_2 and I_3 are integrals of the form:

$$I_1 = \int_{-1}^1 (1+au)^4 du \quad (e)$$

$$I_2 = \int_{-1}^1 (1+au)^4 \ln u^2 du \quad (f)$$

$$I_3 = \int_{-1}^1 (1+au)^4 \ln(1+au) du \quad (g)$$

where "a" is a parameter dependent upon the direction cosine of the normal to the segment, "co", according to the expression:

$$a = -\frac{L \text{ co}}{2R'} \quad (h)$$

and R' and Z' are the coordinates of the middle of the segment. A proper choice of coordinates restricts "a" between -1 and 1.

The integrals in (e)-(g) have the following values:

$$I_1 = \frac{2}{3a} [(1+a)^5 - (1-a)^5] \quad (i)$$

$$I_2 = -\frac{8}{3a} \frac{1}{3} \{-[(1+a)^{3/2} - (1-a)^{3/2}] + [(1+a)^4 - (1-a)^4] + \frac{1}{2} X\} \quad (j)$$

$$\text{where } X = \ln\left[\frac{1+(1-a)}{1-(1-a)}\right] + \ln\left[\frac{(1+a)-1}{(1+a)+1}\right]$$

$$I_3 = -\frac{1}{3}[(1+a)^{3/2}\ln(1+a)-(1-a)^{-3/2}\ln(1-a)] - \frac{2}{9}[(1+a)^{3/2}-(1-a)^{-3/2}] \quad (\text{k})$$

Assembling (i), (j) and (k), we obtain G_{11} .


```

46      display"theta (not a multiple of 9 degrees!)"
        accept the
        display"theta=",the
        if(the.ge.90.or.the.le.0.) go to 44
        if(the.eq.9.or.the.eq.18.or.the.eq.27.or.the.eq.36.
or.the.eq.45.or.the.eq.54.or.the.eq.63.or.the.eq.72.
        or.the.eq.81) go to 46
        go to 45
44      display"theta between 0 and 90 degrees!"
        go to 46
45      th=the*3.1415926/180.
        iap=0
        do=2.
        display"internal radius (default=2.)"
        accept do
        display"internal radius=",do
        ti=3.5
        display"length of protruded part (default=3.5)"
        accept ti
        display"length of protruded part=",ti
        do 10 i=1,10
        alfa(i)=.1570796327*float(i)
        xc(i)=do*sin(alfa(i))
        yc(i)=.5+do*(1.-cos(alfa(i)))
        if(th.gt.alfa(i)) iap=iap+1
10      continue
        xib=do*sin(th)
        yib=.5+do*(1.-cos(th))
        iaq=10-iap
        display"length of cable taken into account: 5x internal
        radius"
        elong=5*do
        do 84 i=1,11
        xa(i)=(1-i)*elong/10.
        xb(i)=-10.-xa(i)
        yb(i)=1.+do
        xa(mra-i+1)=xa(i)
        ya(i)=.5+do
84      ya(mra-i+1)=.5
        xa(12)=xa(11)
        ya(12)=(ya(11)+ya(13))/2
        xb(12)=xb(11)
        yb(12)=.5+do
        yb(13)=yb(12)
        yb(14)=yb(13)
        yb(15)=(1+do)/2
        yb(16)=.5
        yb(17)=do/200.
        xb(13)=6.*ti/7.
        do 21 i=1,4
21      xb(13+i)=ti

```

```

data kodea/10*0,2*1,11*0/
data fia/10*1.,2*0.,11*0./
data kodeb/11*0,-1,5*0/
data fib/10*1.,-1.,5*0,1./
data cx/-1.,-2.,-5.,-7.5/
data cy/4*1.5/
ma=mra+iap
na=mr+iaq
mi=ma+ia
ni=na+ia-1

c
c form boundary elements REGION I
c

do 13 i=1,mi
if(i.le.mra) go to 11
if(i.le.ma) go to 12
x(i)=xib
y(i)=yib
kodel(i)=-1
go to 13
11 x(i)=xa(i)
y(i)=ya(i)
kodel(i)=kodea(i)
fil(i)=fia(i)
go to 13
12 x(i)=xc(i-mra)
y(i)=yc(i-mra)
kodel(i)=0
fil(i)=.0
13 continue
do 601 i=1,mi
if(kodel(i).eq.-1) fil(i)=-1
601 continue
c write(6,1162)
c162 format(11x,"X",10x,"Y",8x,"kode",5x,"fi",//)
c write(6,588)
c88 format(10x,"REGION I",//)
x(mi+1)=x(1)
y(mi+1)=y(1)
do 600 i=1,mi
xm(i)=(x(i)+x(i+1))/2
ym(i)=(y(i)+y(i+1))/2
c write(6,273) x(i),y(i)
c write(6,260) i,xm(i),ym(i),kodel(i),fil(i)
c write(6,274) x(i+1),y(i+1)
600 continue
c60 format(2x,i2,5x,2(f6.2,5x),i2,5x,f6.2)
c73 format(9x,2(f6.2,5x))
c74 format(9x,2(f6.2,5x),/)
xx(mi+1)=x(1)
yy(mi+1)=y(1)
do 311 i=1,mi

```

```

xx(i)=x(i)
yy(i)=y(i)
xxm(i)=xm(i)
311  yym(i)=ym(i)
c
c    calculate G1 and H1
c
do 373 i=1,mi
ho=0.
do 33 j=1,mi
if(i-j) 28,29,28
28  call
inte(xm(i),ym(i),x(j),y(j),x(j+1),y(j+1),h1(i,j),g1(i,j))
h1(i,j)=h1(i,j)/eps1
ho=ho+h1(i,j)
go to 333
29  call inlo(x(j),y(j),x(j+1),y(j+1),g1(i,j))
333  g1(i,j)=g1(i,j)/eps1
33  continue
h1(i,i)=-ho
373  continue
c
c    arrange system of equations ready to be solved REGION I
c
do 57 j=1,mi
if(kodel(j)) 57,61,57
61  do 57 i=1,mi
ch1=h1(i,j)
h1(i,j)=-g1(i,j)
g1(i,j)=-ch1
57  continue
c
c    dfil originally contains the independent coefficients
c    after solution it will contain the values of the system
c    unknowns
c
do 162 i=1,mi
dfil(i)=0.
do 162 j=1,mi-ia
dfil(i)=dfil(i)+g1(i,j)*fil(j)
162  continue
c
c    form boundary elements REGION II
c
x(1)=xb(11)
y(1)=yb(11)
kode2(1)=-1
fi2(1)=-1.
do 14 i=2,ni+1
if(i.le.(ia+1)) go to 15
mc2=ia+iaq+1
if(i.le.mc2) go to 16

```

```

mcl=ia+iaq+mrb-11+1
if(i.le.mcl) go to 17
x(i)=xb(i-mcl)
y(i)=yb(i-mcl)
kode2(i)=kodeb(i-mcl)
fi2(i)=fib(i-mcl)
go to 14
15 x(i)=xib
y(i)=yib
kode2(i)=-1
fi2(i)=-1.
if(i.eq.(ia+1)) go to 63
if(i.eq.(ia+1)) go to 63
go to 14
16 mc=ia+1-iap
x(i)=xc(i-mc)
y(i)=yc(i-mc)
kode2(i)=0
fi2(i)=.0
go to 14
63 kode2(i)=0
fi2(i)=.0
go to 14
17 mc=ia+iaq-11+1
x(i)=xb(i-mc)
y(i)=yb(i-mc)
kode2(i)=kodeb(i-mc)
fi2(i)=fib(i-mc)
14 continue
do 700 i=1,mcl-1
xm(i)=(x(i)+x(i+1))/2
700 ym(i)=(y(i)+y(i+1))/2
x(ni+2)=x(1)
y(ni+2)=y(1)
do 701 i=mcl+1,ni+1
xm(i-1)=(x(i)+x(i+1))/2
701 ym(i-1)=(y(i)+y(i+1))/2
c write(6,289)
c89 format(10x,"REGION II",//)
c do 702 i=1,mcl-1
c write(6,273) x(i),y(i)
c write(6,260) i,xm(i),ym(i),kode2(i),fi2(i)
c02 write(6,274) x(i+1),y(i+1)
c do 703 i=mcl+1,ni+1
c write(6,273) x(i),y(i)
c write(6,260) i-1,xm(i-1),ym(i-1),kode2(i-1),fi2(i-1)
c03 write(6,274) x(i+1),y(i+1)
c
c calculate G2 and H2
c
do 390 i=1,ni
ho=0.

```

```

do 303 j=1,ni
  l7=j
  if(j.ge.mc1) l7=l7+1
  if(i-j) 20,25,20
20  call
  inte(xm(i),ym(i),x(l7),y(l7),x(l7+1),y(l7+1),H2(i,j),
    1  g2(i,j))
  ho=ho+h2(i,j)
  go to 303
25  call inlo(x(l7),y(l7),x(l7+1),y(l7+1),g2(i,j))
303  continue
  h2(i,i)=-ho+4*3.1415926
390  continue
c
c  arrange system of equations ready to be solved
c
do 50 j=1,ni
  if(kode2(j)) 50,40,50
40  do 50 i=1,ni
  ch=h2(i,j)
  h2(i,j)=-g2(i,j)
  g2(i,j)=-ch
50  continue
c
c  dfi2 originally contains the independent coefficients
c  after solution it will contain the values of the system
c  unknowns
c
do 60 i=1,ni
  dfi2(i)=0.
  do 60 j=ia+1,ni
  dfi2(i)=dfi2(i)+g2(i,j)*fi2(j)
60  continue
c
c  solution of the combined system of equations
c
do 499 i=1,ni+mi
  do 499 j=1,ni+mi
499  ht(i,j)=0.0
c
c  upper part
do 132 j=1,mi
  do 132 i=1,mi
  ht(i,j)=h1(i,j)
132  continue
c
c  lower part
l4=mi-ia
l3=mi+ni
do 232 j=l4+1,l3-ia
  do 232 i=mi+1,l3
  ht(i,j)=+h2(i-mi,j-l4)

```

```

232     continue
c
c     add band of G intern
c
c     upper part
do 332 j=13+1-ia,13
do 332 i=1,mi
332     ht(i,j)=-g1(i,j-ni)
c
c     lower part
l5=0
do 432 j=13+1-ia,13
l5=l5+1
do 432 i=mi+1,13
432     ht(i,j)=+g2(i-mi,l5)*eps1/eps2
do 179 i=1,mi+ni
if(i.le.mi) go to 79
dfi(i)=dfi2(i-mi)
kode(i)=kode2(i-mi)
fi(i)=fi2(i-mi)
go to 179
79     dfi(i)=dfi1(i)
kode(i)=kode1(i)
fi(i)=fi1(i)
179     continue
call slnpd(ht,dfi,d,mi+ni,nx)
c
call inter(fi,dfi,kode,cx,cy,xx,yy,sol)
c
output
c
call outpt(xxm,yym,fi,dfi,cx,cy,sol,xm,ym)
stop
end

c
$control bounds
subroutine inte(xp,yp,x1,y1,x2,y2,h,g)
c
c     this subroutine computes the values of the G and H matrix
off-diagonal elements by means of numerical integration
along boundary elements
c
c
dimension xco(4),yco(4),gi(4),ome(4)
gi(1)=0.86113631
gi(2)=-gi(1)
gi(3)=0.33998104
gi(4)=-gi(3)
ome(1)=0.34785485
ome(2)=ome(1)
ome(3)=0.65214515

```

```

ome(4)=ome(3)
ax=(x2-x1)/2.
bx=(x2+x1)/2.
ay=(y2-y1)/2.
by=(y2+y1)/2.
if(abs(ay).le..0001) go to 300
ta=-ax/ay
dim=sqrt(ta**2+1.)
if(ay.gt.0.) dim=-dim
if(abs(dim).ge.50000.) pause"dim too big!"
co=1/dim
si=ta*co
go to 39
300 co=0.
    si=1.
    if(ax.lt.0.) si=-si
39  g=0.
    h=0.
    do 40 i=1,4
    xco(i)=ax*gi(i)+bx
    yco(i)=ay*gi(i)+by
    a=yp**2+yco(i)**2+(xp-xco(i))**2
    b=2*yp*yco(i)
    am=2*b/(a+b)
    call ellip(am,ak,ae)
    g=g+4*ak/sqrt(a+b)*ome(i)*sqrt(ax**2+ay**2)*yco(i)
    ft=(yp**2-yco(i)**2+(xp-xco(i))**2)*ae/(a-b)-ak
    st=yco(i)*(xp-xco(i))*ae/(a-b)
40  h=h-4/sqrt(a+b)*(ft/2*si+st*co)*ome(i)*sqrt(ax**2+ay**2)
    return
end

```

```

c
$control bounds
  subroutine inlo(x1,y1,x2,y2,g)
c
c   this subroutine calculates the diagonal elements of G
c
  ax=x2-x1
  ay=y2-y1
  bx=(x2+x1)/2
  by=(y2+y1)/2
  alen=sqrt(ax**2+ay**2)
  if(abs(ay).le.0.0001) go to 300
  a=.0
  ta=-ax/ay
  dim=sqrt(1+ta**2)
  if(ay) 12,12,10
10  dim=-dim
12  co=1/dim
    si=ta*co

```

```

c      co=nz
c      si=nr
      a=-co*alen/(2*by)
      if(abs(a).ge.1.) display "a greater than one!"
      ap=sqrt(1+a)
      am=sqrt(1-a)
      gv1=(ap**3-am**3)*(2/?-alog((alen/(16*by))**2))
      gv2=alog(abs((1+am)/(1-am)))+alog(abs((ap-1)/(ap+1)))
      gv3=ap-am
      gv4=(ap**3)*alog(ap**2)-(am**3)*alog(am**2)
      g=alen/(3*a)*(gv1+2*gv2+4*gv3+gv4)
c
      return
300    g=alen*(2.-alog'(alen/(16*by))**2))
      return
      end

```

```

c
c
$control bounds
      subroutine slnprd(a,b,d,n,ny)
c
c      solution of linear sys
      dimension a(ny,ny), b(ny)
      n1=n-1
      do 100 k=1,n1
      k1=k+1
      c=a(k,k)
      if(abs(c)-0.000001) 1,1,3
1      do 7 j=k1,n
      if(abs(a(j,k)-0.000001)) 7,7,5
5      do 6 l=k,n
      c=a(k,l)
      a(k,l)=a(j,l)
6      a(j,l)=c
      c=b(k)
      b(k)=b(j)
      b(j)=c
      c=a(k,k)
      go to 3
7      continue
8      write(6,2) k
2      format(1x,"*****singularity in row",i5)
      d=0.
      go to 300
3      c=a(k,k)
      do 4 j=k1,n
4      a(k,j)=a(k,j)/c
      b(k)=b(k)/c
      do 10 i=k1,n
      c=a(i,k)

```

```

          do 9 j=k1,n
9         a(i,j)=a(i,j)-c*a(k,j)
10        b(i)=b(i)-c*b(k)
100       continue
          if(abs(a(n,n))-0.000001) 8,8,101
101      b(n)=b(n)/a(n,n)
          do 200 l=1,n1
          k=n-1
          k1=k+1
          do 200 j=k1,n
200      b(k)=b(k)-a(k,j)*b(j)
          d=1.
          do 250 i=1,n
250      d=d*a(i,i)
300      return
          end

```

\$control bounds

```

          subroutine inter(fi,dfi,kode,cx,cy,xx,yy,sol)
c
c      reorder fi and dfi arrays to put all the values of the
          potential in fi and all the values of the derivatives in
          dfi
          common nx,ma,na,ia,iap,iaq,li,mi,ni,eps1,eps2
          dimension fi(55),dfi(55),kode(55),cx(5),cy(5)
          dimension sol(5),xx(35),yy(35)
          l8=mi-ia
          do 20 i=1,l8
          if(kode(i)) 20,20,10
10         ch=fi(i)
          fi(i)=dfi(i)
          dfi(i)=ch
20        continue
c
          do 44 i=1,ia
          fi(i+l8)=dfi(i+l8)
          fi(mi+i)=dfi(i+l8)
44        dfi(l8+i)=dfi(ni+l8+i)
          do 59 i=1,ni-ia
          dfi(mi+ni+1-i)=dfi(ni+l8+1-i)
59        do 53 i=1,ia
          dfi(mi+i)=dfi(l8+i)
          do 45 i=mi+1+ia,ni+mi
          if(kode(i)) 45,45,48
48        ch=fi(i)
          fi(i)=dfi(i)
          dfi(i)=ch
45        continue
c      compute potential at internal points
          do 40 k=1,li
          sol(k)=0.

```

```

do 30 j=1,mi
call inte(cx(k),cy(k),xx(j),yy(j),xx(j+1),yy(j+1),a,b)
30 sol(k)=sol(k)+dfi(j)*b-fi(j)*a
40 sol(k)=sol(k)/(4*3.1415926)
return
end
$control bounds
subroutine outpt(xxm,yym,fi,dfi,cx,cy,sol,xm,ym)
common nx,ma,na,ia,iap,iaq,li,mi,ni,eps1,eps2,do
dimension xxm(35),yym(35),fi(55),dfi(55),cx(5)
dimension xm(35),ym(35),cy(5),sol(5)
write(6,202)
write(6,202)
202 format(/)
WRITE (6,201)
201 FORMAT(5X,"X",16X,"Y",16X,"POTENTIAL",8X,"POTENTIAL
DERIVATIVE")
write(6,202)
write(6,202)
display " REGION I"
write(6,202)
write(6,202)
do 10 i=1,mi-ia
10 write(6,200) xxm(i),yym(i),fi(i),dfi(i)
200 format(4(3x,e14.7))
write(6,202)
l8=mi-ia
display" internal boundary"
write(6,202)
write(6,202)
do 14 i=1,ia
14 write(6,200) xxm(l8+i),yym(l8+i),fi(l8+i),dfi(l8+i)
write(6,202)
write(6,202)
write(6,202)
display " REGION II"
write(6,202)
write(6,202)
do 15 i=ia+1,ni
15 write(6,200) xm(i),ym(i),fi(mi+i),dfi(mi+i)
write(6,202)
write(6,202)
write(6,203)
203 format(2x,"INTERNAL
POINTS",//,11X,"X",18x,"Y",14x,"POTENTIAL")
do 20 k=1,li
20 write(6,204) cx(k),cy(k),sol(k)
204 format(3(5x,e14.7))
sigma1=.0
sigma2=.0
do 33 i=1,10
sigma1=sigma1+dfi(i)

```

```

33      sigma2=sigma2+dfi(ni+mi-i)
        c1=dc+.5
        c2=do+1.
        sigma=c1*sigma1*eps1/2.+eps2*(c2*sigma2/2.+(c2**2
&      -c1**2)*dfi(ni+mi)/4.)
        sigma=sigma*8.85
c      write(6,92) sigma
c2     format(5x,"charge on upper conductor=",f14.6,"nC",//)
        write(6,93) sigma
93     format(5x,"capacitance of system=",f14.6,"pF",//)
        return
        end

```

\$control bounds

```

C      Polynomial Approximations of Elliptic Integrals of
c      the First and Second Kinds
C

```

```

subroutine ellip(m,kk,ke)
dimension a(2,5),b(2,5),as(5),bs(5)
real m,m1,m2,k,k1,kk,ke
a(1,1)=1.38629436112
a(1,2)=0.09666344259
a(1,3)=0.03590092383
a(1,4)=0.03742563713
a(1,5)=0.01451196212
b(1,1)=.5
b(1,2)=.12498593597
b(1,3)=.06880248576
b(1,4)=.03328355346
b(1,5)=.00441787012
a(2,1)=1.
a(2,2)=.44325141463
a(2,3)=.06260601220
a(2,4)=.04757383546
a(2,5)=.01736506451
b(2,1)=0.0
b(2,2)=.24998368310
b(2,3)=.09200180037
b(2,4)=.04069697526
b(2,5)=.00526449639
m1=1.-m
m2=1./m1
do 10 i=1,2
do 11 j=1,5
as(j)=a(i,j)
11 bs(j)=b(i,j)
k=(as(1)+as(2)*m1+as(3)*m1**2+as(4)*m1**3+as(5)*m1**4)
k1=(bs(1)+bs(2)*m1+bs(3)*m1**2+bs(4)*m1**3+bs(5)*m1**4)*alog(m2)
if(i.eq.2) go to 33
kk=k+k1

```

```
33      go to 10  
10      ke=k1+k  
        continue  
        return  
        end
```

REFERENCES

- [1] C.A. Brebbia, "The Boundary Element Method for Engineers," London, Pentech Press 1980
- [2] R. E. Collin and D. A. Ksienski, "Boundary Element Method for dielectric resonators and waveguides," Radio Sci. (USA), 22(7), pp. 1155-67, Dec. 1987
- [3] R. F. Milson and K. J. Scott, "RF simulation of complex layout by quasistatic Boundary Element Method," IEE, p. 13/1-7, 1987
- [4] K. Miyata and I. Fukai, "A cylindrical reflector antenna pattern computation by the Boundary Element Method," IEEE, Vol. 1, pp. 492-5, 1987
- [5] T. Misaki, H. Tsuboi and Y. Kawakami, "An analysis of three-dimensional eddy-current distribution by means of the Boundary Element Method", Electr. Eng. Jpn (USA), 105(6), pp. 30-7, Nov-Dec. 1985
- [6] D. A. Christiansen and C. H. Durney, "Hyperthermia production for cancer therapy: a review of fundamentals and methods", J. Microwave Power, Vol. 16, No. 2, pp. 89-105, June 1981

[7] L. E. Larsen and J. H. Jacobi, "Microwave scattering parameter imagery of an isolated canine kidney", *Med. Phys.*, Vol. 6, No. 5, pp. 394, 1979

[8] E. H. Grant, R. J. Sheppard and G. P. South, "Dielectric behaviour of biological molecules in solution", Clarendon Press, Oxford 1978

[9] E. C. Burdette, F. L. Cain and J. Seals, "In-vivo probe measurement technique for determining dielectric properties at VHF through microwave frequencies", *IEEE Trans. Microwave Theory Tech.*, Vol. IM-28, No. 4, April 1980

[10] E. Tanabe and W. T. Jones, "A nondestructive method for measuring the complex permittivity of dielectric materials at microwave frequencies using an open transmission line resonator", *IEEE Trans. Instrum. Meas.*, Vol. IM-25, pp. 222-6, 1976

[11] W. B. Westphal, "Dielectric measuring techniques" in *Dielectric Materials and Applications*, A. R. von Hippel Ed., New York: Wiley, pp. 63-122, 1954

[12] S. Roberts and A. von Hippel, "A new method for measuring dielectric constant and loss in the range of centimetre waves", *J. Appl. Phys.*, Vol. 17, pp. 610-6, 1946

- [13] M. A. Stuchly and S. S. Stuchly, "Coaxial line reflection methods for measuring dielectric properties of biological substances at radio and microwave frequencies - a review", IEEE Trans. Instrum. Meas., Vol. IM-29, No. 3, pp. 176-83, 1980
- [14] K. P. A. P. Esselle, "New fringe-field capacitive sensors", M. Sc. (Electrical engineering) thesis, University of Ottawa, 1987.
- [15] S. S. Stuchly, M. A. Rzepecka and M. F. Iskander, "Permittivity measurements at microwave frequencies using lumped elements", IEEE Trans. Instrum. Meas., Vol. IM-23, pp. 56-62, 1974
- [16] M. F. Iskander and S. S. Stuchly, "Fringing field effect in the lumped capacitance method for permittivity measurements", IEEE Trans. Instrum. Meas., Vol. IM-27, pp. 107-9, 1978
- [17] Hugo Fellner-Feldeg, "The Measurement of Dielectrics in the Time Domain", J. Phys. Chem., Vol. 73, No. 3, pp. 616-23, 1969
- [18] R. H. Cole, "Evaluation of Dielectric Behavior by Time Domain Spectroscopy", J. Phys. Chem., Vol. 79, No. 14, pp. 1459-69, 1975
- [19] R. H. Cole, "Time Domain Reflectometry", Ann. Rev. Phys.

Chem., Vol. 28, pp. 283-300, 1977

[20] R. Chahine and T. K. Bose, "Comparative studies of various methods in time domain Spectroscopy", J. Chem. Phys., Vol. 72, No. 2, pp. 808-815, 1980

[21] N. Markuvitz, "Waveguide Handbook", Dover Publications, Boston Mass., 1955

[22] J. Galejs, "Antennas in inhomogeneous media" Pergamon Press, Oxford, pp. 39-43, 1969

[23] G. Gayda, "Numerical analysis of in-vivo sensors", M. Sc. (Electrical Engineering) thesis, University of Ottawa, 1982

[24] M. M. Ney, "Method of Moments as Applied to Electromagnetic Problems", IEEE, Vol. MTT-33, No. 10: 972-80

[25] C. A. Brebbia, "Boundary Element techniques: theory and applications in Engineering", New York: Springer-Verlag, 1984

[26] A. Ralston, "A first course in numerical analysis", McGraw-Hill, 1965

[27] M. Abramovitz and I. Stegun, "Handbook of Mathematical functions", Dover Publications, 1965

[28] A. Cayley, "An elementary treatise on elliptic functions",
Dover Publications, 1965